



## Development of robotics tools for agricultural task achievement: The example of robot formation control

R. Lenain, P. Cartade, Benoît Thuilot, P. Delmas, M. Berducat

### ► To cite this version:

R. Lenain, P. Cartade, Benoît Thuilot, P. Delmas, M. Berducat. Development of robotics tools for agricultural task achievement: The example of robot formation control. IEEE/RSJ International Conference on Intelligent Robots and Systems, IROS'12, Oct 2012, Vilamoura, Portugal. IEEE, 8 p., 2012. <hal-00766294>

**HAL Id: hal-00766294**

**<https://hal.archives-ouvertes.fr/hal-00766294>**

Submitted on 18 Dec 2012

**HAL** is a multi-disciplinary open access archive for the deposit and dissemination of scientific research documents, whether they are published or not. The documents may come from teaching and research institutions in France or abroad, or from public or private research centers.

L'archive ouverte pluridisciplinaire **HAL**, est destinée au dépôt et à la diffusion de documents scientifiques de niveau recherche, publiés ou non, émanant des établissements d'enseignement et de recherche français ou étrangers, des laboratoires publics ou privés.

# Development of Robotics Tools for Agricultural Task Achievement: The example of robot formation control

Roland Lenain<sup>1</sup>, Pierre Cartade<sup>1</sup>, Benoit Thuilot<sup>2,3</sup>, Pierre Delmas<sup>1</sup>, Michel Berducat<sup>1</sup>

**Abstract**—Nowadays it is eagerly expected that, on one hand the environmental impact of agricultural activities is decreasing, and on the other hand the level of production is increasing in order to match the consumption demand of the growing worldwide population. To meet these opposite expectations, new production tools have to be developed. Recent advances in off-road mobile robotics may bring to promising solution in order to address such a problematic. Since large area coverage, as well as high flexibility, are more particularly looked for in this paper, multi-robot cooperation for field operations is investigated.

The proposed framework relies on a path tracking approach dedicated to the formation control of several robots. In an off-road context, because of bad grip conditions, classical control algorithms cannot be used straightforwardly. Moreover, low level delays and stability issues (rollover risk or obstacle collision) have also to be taken into account. Adaptive and predictive control laws are here designed to achieve accurate motion control of each robot, despite highly varying and unpredictable contact conditions. The multi-robot configuration is imposed by defining set points in terms of lateral deviations and longitudinal distances between each robot. In addition, robot safety is addressed through a traversability evaluation within the vicinity of each robot. Finally, several alternative paths are constantly considered and the optimal one is decided with respect to robot stability and maximal velocity criteria, assessed from a numerical terrain model.

## I. INTRODUCTION

The recent progress in the motion control of mobile robots (concerning both a single robot [1], as well as multi-robots [2], [3]) makes possible to consider new devices in several different applications. For instance, the use of mobile robot cooperation in order to address the task of large area covering [4] is of interest to solve many problems in many fields such as surveillance, cleaning, exploration, etc. In particular, environmental applications like farming may benefit from improvement of off-road robotics research. As it is stated in [5], the accuracy improvement in off-road robot control may provide new solutions to reduce environmental impact while preserving a high level of production. Instead of using numerous small robots, as it is investigated in swarm robotics research [6], this paper favors a cooperation framework with a limited number of light machines. Such a strategy indeed seems more realistic in the middle term:

<sup>1</sup>Irstea, TSCF Unit, Centre of Clermont-Ferrand, 24 avenue des Landais BP50085, Aubiere Cedex, France [roland.lenain@irstea.fr](mailto:roland.lenain@irstea.fr)

<sup>2</sup>B. Thuilot is with Institut Pascal, Université Blaise Pascal, BP 10448, 63000 Clermont-Ferrand, France

<sup>3</sup>B. Thuilot is also with CNRS - UMR 6602, 63177 Aubiere, France [benoit.thuilot@lasmea.univ-bpclermont.fr](mailto:benoit.thuilot@lasmea.univ-bpclermont.fr)

This work is supported by French National Research Agency (ANR), under the grant ANR-07-ROBO-0008 attributed to the finished FAST project, extended with the grant ANR-10-VPTT-011 attributed to SafePlatoon Project.

on one hand, some farming operations such as harvesting require quite large machines to achieve tasks properly, and on the other hand, it appears more tractable from a practical point of view (maintenance, monitoring, acceptability, etc). In this paper, the formation control of several light robots is investigated through the trajectory control problem. The target is fields covering using autonomous robots (instead of manually driven ones, see figure 1) in order to achieve agriculture tasks. This allows the use of several autonomous entities instead of driving a sole huge vehicle, and the possibility to retain one master vehicle driven manually.



Fig. 1. Illustration of the targeted application

This problem is then addressed by considering a reference path, previously learned (by a manual driving or by computation) or achieved on-line by the first vehicle driven manually. A desired shape for the robots configuration is then defined in the trajectory frame (in terms of curvilinear distance between robots along the reference path and lateral deviation with respect to this trajectory). The configuration is not considered as frozen but potentially variable since several tasks are targeted (field covering, machine unloading, platooning). The proposed work then aims at servoing the robots such as they achieve the desired configuration. Several approaches have been proposed for mobile robot formation control [7], [8], but are mainly dedicated to structured environments. In contrast, the context of the considered tasks requires a high accurate relative positioning of the robots despite the numerous perturbations encountered in natural environment (skidding, terrain irregularities, etc).

In this paper, an adaptive algorithm for formation control is proposed, relying on a reference trajectory defining a local relative frame. It decouples longitudinal and lateral dynamics

with respect to the desired path: the advance of each robot along the reference path can be addressed independently from the regulation of its lateral deviation with respect to this path. Longitudinal control is based on the regulation of curvilinear inter-vehicle distances, while lateral regulation relies on an observer-based adaptive control approach. The control of the possibly varying formation gathers both control laws, enabling an accurate formation regulation for field operations, independently from the reference path shape and environment properties.

Above the high level of accuracy required to enable a relevant agricultural work, it is necessary to ensure the robot safety too. In particular, autonomous robots must avoid collision, between themselves and with elements of the environment. Many researches are interested in obstacle avoidance for mobile robots [9], [10], but they rely on a binary vision of the environment. As a result, some difficult areas, crossable at reduced speed are avoided and the robot stability has still to be addressed. In this paper, both stability preservation and obstacle avoidance are addressed considering the notion of traversability [11]. Considering the availability of a digital elevation map, the maximal admissible velocity through the environment guaranteeing robot integrity (in terms of rollover risk and maximal admissible angular velocity and acceleration) is computed. It permits to unify obstacle avoidance and stability preservation since an obstacle is just an area crossable at a null velocity.

The paper is organized as follows. A model dedicated to a mobile robot formation is first introduced, together with the observation strategy allowing to reflect the bad grip conditions encountered in natural environment. Based on this model, the control of each mobile robot is then detailed: longitudinal control is recalled from previous work, while lateral control is designed with respect to a varying set point, associated to predictive control principles. In addition, the integrity preservation is studied thanks to the maximal admissible speed, evaluated along several alternative trajectories. A minimization algorithm then permits to select the optimal trajectory and the desired velocity. The validation of the proposed control is finally performed thanks to actual experiments achieved in off-road conditions using autonomous mobile robots.

## II. ROBOT FORMATION MODELING FOR MOTION CONTROL

### A. Extended kinematic model of robots

The framework proposed in this paper for proceeding the motion control of each robot is based on the model depicted in figure 2. For simplicity reasons, only two robots  $i$  and  $i+1$  are shown among  $n > 2$  robots.

In the model shown on figure 2, each robot is considered as a bicycle, i.e. a unique wheel stands for the front axle and another one for the rear one (standard Ackermann representation, see [12]). Nevertheless, since bad grip conditions cannot be ignored in natural environment, this model differs from classical approaches in that two sideslip angles are considered:  $\beta^F$  and  $\beta^R$ , respectively for front and rear axles.

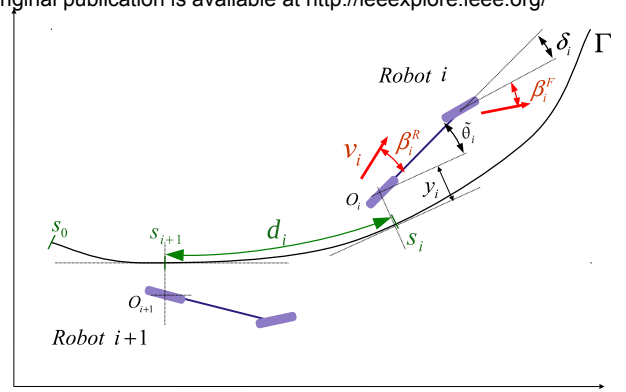


Fig. 2. Extended kinematic model dedicated to formation control

The use of model assuming rolling without sliding condition indeed leads to large errors (see [13]) not satisfying considering the farm tasks requirement. Sideslip angles then permit to account for perturbations due to the tire-ground interaction without relying on complete dynamical models (such as defined in [14]), since these latter require the knowledge of numerous parameters. The advantage of this modeling is that control design can still be derived relying on the efficient approaches proposed when rolling without sliding assumptions are valid. These variables are representative of the difference between the tire orientation and the actual tire speed vector direction. They are here input in this model in order to be observable (their estimation is indeed described in section II-B). Longitudinal sliding is neglected in this paper, considering a limited speed for robots (around 2m/s), and that longitudinal accuracy is not as critical as the lateral precision (a discussion about the longitudinal accuracy is detailed in conclusion). Based on these assumptions, the notations used in the sequel are depicted in figure 2 for the  $i^{th}$  robot and hereafter listed:

- $\Gamma$  is the common reference path for each robot defined in an absolute frame (computed or recorded beforehand).
- $O_i$  is the center of the  $i^{th}$  mobile robot rear axle. It is the point to be controlled for each robot.
- $s_i$  is the curvilinear coordinate of the closest point from  $O_i$  belonging to  $\Gamma$ . It corresponds to the distance covered along  $\Gamma$  by robot  $i$ .
- $c(s_i)$  denotes the curvature of path  $\Gamma$  at  $s_i$ .
- $\theta_i$  denotes the angular deviation of robot  $i$  w.r.t.  $\Gamma$ .
- $y_i$  is the lateral deviation of robot  $i$  w.r.t.  $\Gamma$ .
- $\delta_i$  is the  $i^{th}$  robot front wheel steering angle.
- $l_i$  is the robot wheelbase.
- $v_i$  is the  $i^{th}$  robot linear velocity at point  $O_i$ .
- $\beta_i^F$  and  $\beta_i^R$  denote the sideslip angles (front and rear) of the  $i^{th}$  robot.

Using these notations, the motion equations for the  $i^{th}$

mobile robot can be expressed as (see [15] for details):

$$\begin{aligned} \dot{s}_i &= v_i \frac{\cos(\tilde{\theta}_i + \beta_i^R)}{1 - c(s_i) y_i} \\ \dot{y}_i &= v_i \sin(\tilde{\theta}_i + \beta_i^R) \\ \dot{\tilde{\theta}}_i &= v_i \left( \cos \beta_i^R \frac{\tan(\tilde{\theta}_i + \beta_i^R) - \tan(\beta_i^R)}{l_i} - \frac{c(s_i) \cos \tilde{\theta}_i}{1 - y_i c(s_i)} \right) \end{aligned} \quad (1)$$

Expression (1) does not exist if  $[1 - c(s_i)y_i] = 0$  (i.e. point  $O_i$  is superposed with the instantaneous reference path center of curvature). Such a situation is not encountered in practice, since robots are supposed to be properly initialized. The state vector for robot  $i$  is then defined as  $X_i = [s_i \ y_i \ \tilde{\theta}_i]^T$ , and is supposed to be measured. As a result, model (1) is entirely known as soon as sideslip angles  $\beta_i^F$  and  $\beta_i^R$  are accessible. As these variables cannot be easily measured, they are estimated thanks to an observer described below.

### B. Sideslip angles estimation

As sideslip angles integrated into robot model (1) are hardly measurable directly, their indirect estimation has to be addressed. The observer-based approach detailed in [16] is here implemented. The proposed algorithm, described in figure 3, takes benefit of the duality principle between observation and control.

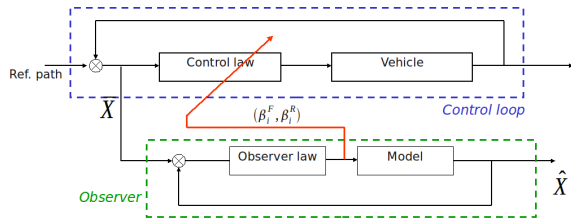


Fig. 3. Observer principle scheme

More precisely, model (1) can be viewed as representative if its outputs ( $y_i$  and  $\tilde{\theta}_i$ ) converge to the corresponding measured variables. As a result, the model is considered to be a process whose inputs are the sideslip angles and a control law is designed for these latter in order to impose that the lateral and angular deviations ( $X_i^{obs} = [y_i^{obs} \ \tilde{\theta}_i^{obs}]^T$ ) computed by the model (1) converge to the corresponding measurements ( $\bar{X}_i = [\bar{y}_i \ \bar{\theta}_i]^T$ ). Such a convergence ensures that model (1) is representative of vehicle actual behavior whatever the grip conditions, and sideslip angle values can then be reported into mobile robot control laws. The detailed computation of this observer and the proofs of stability are available in [16].

## III. ROBOT CONTROL

### A. Motion control

Since the perception system detailed in section IV-A, together with the observer previously described, permit to measure or estimate all of the variables, the model (1) is entirely known. Accurate motion control of the robot formation can then be addressed, while preserving a simple kinematic structure, allowing to tackle almost independently longitudinal and lateral motion.

1) *Longitudinal control*: The objective of longitudinal control is to maintain a desired distance (denoted  $d$ ) between curvilinear abscissas of successive vehicles. Preferentially, each robot is controlled with respect to the curvilinear abscissa  $s_1$  of the leader ( $1^{st}$  vehicle). This enables to avoid an oscillating behavior due to error propagation along the fleet. However, for obvious safety reasons, the distance to the previous vehicle has also to be considered. Therefore, as proposed in [17], a composite error  $x_i$  equal to the distance to the leader vehicle  $e_i^1$  in the nominal case, and smoothly commuting to the distance to the preceding vehicle  $e_i^{i-1}$  when the security distance is approached, is here regulated, see figure 4. The control law  $v_i$  ensuring that  $x_i$  converges with zero can easily be designed from the first equation in model (1), so that each vehicle can be accurately and safely controlled longitudinally, whatever the velocity of the leader.

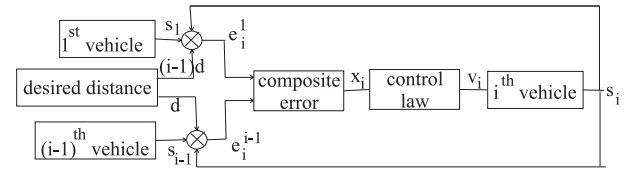


Fig. 4. Longitudinal control scheme

2) *Adaptive lateral control*: Once longitudinal control has been achieved, the control of the lateral position of each robot can be addressed. Despite the addition of sideslip angles, the model (1) is still consistent with a classical mobile robot model and can then be turned into a linear chained form (see [12]). Nevertheless, in contrast to the classical path tracking problem, where the tracking error is expected to be null [18], the lateral deviation of each robot in a formation has here to converge to a non-null desired set point  $y_i^d$ . Convergence of  $y_i$  to  $y_i^d$  can be achieved by imposing the control law (2) detailed in [19]:

$$\delta_i = \arctan \left[ \tan(\beta_i^R) + \frac{l_i}{\cos(\beta_i^R)} \left( \frac{c(s_i) \cos \gamma_i}{\alpha_i} + \frac{A_i \cos^3 \gamma_i}{\alpha_i^2} \right) \right] - \beta_i^F \quad (2)$$

$$\text{where : } \begin{cases} \gamma_i &= \tilde{\theta}_i + \beta_i^R \\ \alpha_i &= 1 - c(s_i) y_i \\ \eta_i &= \tan \gamma_i - \frac{y_i^d}{v_i \cos \gamma_i} \\ A_i &= -K_p \epsilon_i^y - K_d \alpha_i \eta_i + c(s_i) \alpha_i \tan^2 \gamma_i \end{cases}$$

Control law (2) exists under the following assumptions:

- the longitudinal acceleration can be neglected ( $\dot{v}_i = 0$ ).
- $1 - c(s_i)y_i \neq 0$ : model existence condition, already discussed.
- $\gamma_i \neq \frac{\pi}{2}[\pi]$ , i.e. the rear robot speed vector is not perpendicular to the path to be followed. It is satisfied when the formation is properly initialized.

The variable  $d_i$  permits to define the distance between robots within the fleet and then their relative longitudinal

positions. In the same way,  $y_i^d$  in (2) permits to define their lateral positions with respect to the overall formation motion. Longitudinal and lateral relative positions of each robot can then be specified in the reference trajectory frame independently.

3) *Predictive curvature servoing*: As shown in [15], the settling time of the steering angle actuator as well as mobile robot inertia generate overshoots in lateral servoing, when the reference path curvature varies. As achieved in the above mentioned reference, it is possible to anticipate for such variations by using, on curvature servoing, a model predictive control based approach. Similarly to [15], the control law (2) can be split into two terms, such as:

$$\delta_i = \delta_i^{Deviation} + \delta_i^{Traj} \quad (3)$$

where  $\delta_i^{Deviation}$  is mainly dedicated to reduce the lateral error induced by sliding effects, when  $\delta_i^{Traj}$  deals with the curvature servoing (i.e., imposes that the curvature of the robot converges to the curvature of the reference path corrected from the desired lateral deviation). From a theoretical point of view, when there is no perturbation due to unpredictable sideslip angles, the second term in (3) should be:

$$\delta_i^{Traj} = L \frac{c(s_i)}{1 - c(s_i)y_i^d} \quad (4)$$

It can be predicted from the knowledge of the entire reference trajectory. Let us consider a distance of prediction  $s_i^h$  for robot  $i$  corresponding to the distance achieved during the settling time  $T_i^h$  of the steering angle actuator, such as:

$$s_i^h = v_i T_i^h \quad (5)$$

From the knowledge of the reference path, a future set point for the curvature servoing part of the control law can be anticipated (sliding effects are supposed to be addressed by the reactive part  $\delta_i^{Deviation}$ ):

$$T_{target} \delta_i^{Traj} = L \frac{c(s_i + s_i^h)}{1 - c(s_i + s_i^h)y_i^d} \quad (6)$$

Then, relying on predictive control techniques, a set of successive control values over the horizon  $T_i^h$  is computed with the aim of minimizing the difference between a desired steering angle time evolution leading to  $T_{target} \delta_i^{Traj}$  and the expected steering angle time evolution computed from the actuator model. The first element of this set, denoted  $\delta_i^{Pred}$  is then substituted for  $\delta_i^{Traj}$  in 3, so that the predictive control law is eventually:

$$\delta_i = \delta_i^{Deviation} + \delta_i^{Pred} \delta_i^{Traj} \quad (7)$$

This modified control law permits to anticipate for curvature variation and finally limits the possible overshoots encountered, preserving the accuracy whatever the shape of the reference trajectory.

## B. Traversability evaluation

1) *Generation of alternative path*: Since motion control is referred to a desired (and possibly varying) lateral deviation  $y^d$  defining the formation shape, this variable may be used

to avoid an uncrossable area in front of one of the robots. As a result, in order to anticipate for a potential necessary deviation from the reference trajectory, a set of offsets is defined. For instance, on figure 5, a set of 6 offsets uniformly spaced from -0.5m to 2.5m are considered, so that the candidate trajectories stay within  $\pm 2m$  corridor around the reference path. Next, in order to meet robot capabilities,

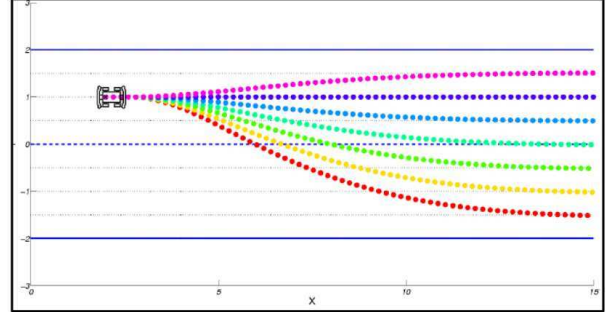


Fig. 5. Alternative trajectory in order to avoid a non crossable area

functions for the desired lateral deviation  $y^d$  allowing to reach one of the offsets are defined with respect to the curvilinear abscissa for each of the offsets, so that eventually a set of local trajectories dedicated to the avoidance of hardly crossable area is available.

2) *Maximal admissible speed computation*: The objective is here to derive the maximal admissible velocity profiles along the initial and alternative trajectories. This permits on one hand to adapt in real time the robot speed in order to ensure the robot static stability, and on the other hand to possibly propose to follow an alternative path limiting the speed reduction. The maximal speed computation is based on the analysis of geometric stability and maximal inclination variation from an available digital elevation map (the production of which is not addressed in this paper). Once an elevation map is derived in front of the robot, its projection along the reference and alternative trajectories can be computed, supplying the roll and pitch angle and their variation. From the robot geometric properties (centre of gravity elevation, width, wheelbase), the projection of the centre of gravity onto the support polygon can be computed along the trajectories and binary obstacles are then identified if this projection crosses the support polygon border. In addition, from roll and pitch angle variations, the longitudinal velocity leading to some specified maximal angular velocity of the robot can be also computed along the trajectories. If the velocity profile along one trajectory reaches zero, this means that such a trajectory cannot be selected due to the presence of an uncrossable area. If all velocity profiles contain a zero, none of the trajectories can be chosen and the robot has to stop.

3) *Desired lateral deviation and velocity selection*: Once the velocity profiles along the initial and alternative trajectories are available, a criterion mixing velocity requirements (the closer to the nominal speed, the better) and lateral deviation (the closer to the reference trajectory, the better) is

evaluated, and the optimal trajectory is eventually selected, so that the robot can move safely, as fast as possible, and the closest to its reference trajectory.

#### IV. EXPERIMENTAL RESULTS

##### A. Experimental testbed

In order to investigate in real conditions the capabilities of the proposed approach, the two mobile robots depicted in figure 6 are used (robots are named RobuFAST and Arocco). Both are electric vehicles, designed for off-road mobility (they are able to climb longitudinal slopes up to  $45^\circ$ ). They are equipped with four independent motors and two steering axles. Their chassis are similar, but their main characteristics



Fig. 6. reference trajectory and actual path achieved by robots

are quite different, see table I. Nevertheless, the control law settings are the same on both robots, demonstrating the robustness of the approach with respect to robot weight and contact patches. In order to feed control laws, several sensors are installed on-board. For motion control, a single RTK-GPS is used, supplying the absolute position of the antenna with an accuracy of  $\pm 2\text{cm}$ . The antenna is settled up to the middle of the rear axle, so that the location of  $O_i$  (see figure 2) is directly available. If such a sensor is sufficient for motion control, communication between robots has also to be considered in order to implement formation control: WLAN communication has here been used. In addition, the elevation map required to evaluate the traversability for each robot is built relying on fusion techniques applied to camera and laser rangefinder data (see [20] for more details).

Robots	RobuFAST	Arocco
Total mass	420kg	620kg
Wheelbase	1.2m	1.2m
Maximum speed	8m/s	3.5m/s
wheel length	5cm	15cm

TABLE I

MAIN PROPERTIES OF CONSIDERED ROBOTS FOR EXPERIMENTS

##### B. Formation control results

In order to validate the proposed formation control approach, path tracking with respect to the path depicted in black line in figure 7 has been considered. This path has been recorded beforehand, when the robot was steered manually

at 1m/s. It is composed of two straight lines and a turn. Half of the trajectory is on a sloping ground (the slope is roughly  $15^\circ$  as shown in figure 6), and the other part on an even ground. On the following figures, one iteration corresponds to 0.1 s.

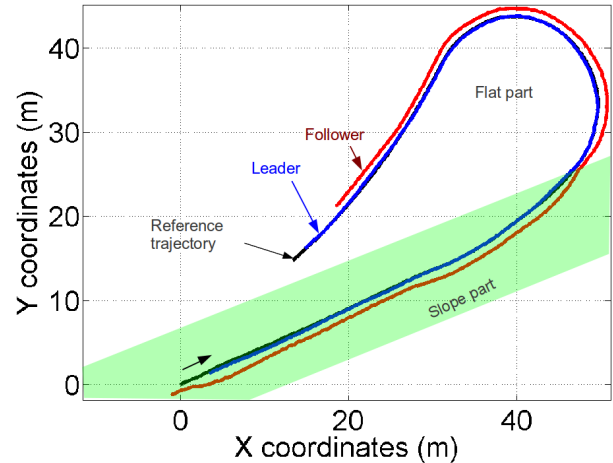


Fig. 7. reference trajectory and actual path achieved by robots

The first robot (considered as a leader) moves at a constant speed equal to 2m/s and its lateral control objective is to follow the reference trajectory. The second robot has to maintain a desired lateral deviation of 1 m with respect to the reference path and a longitudinal distance of 10 m with respect to the leader. The lateral deviations recorded during formation control are reported in figure 8 (blue dotted line for the first robot and red plain line for the second). It can be seen that after an initializing phase (up to iteration 280) the lateral error does not exceed 20 cm with respect to the desired deviations. For the first robot, a small overshoot can be observed around iteration 400. This corresponds to the shock due to the transition between slope and flat ground. This indeed generates a roll motion, and therefore an important translation for the GPS antenna. Since this latter has been settled 1.2m up to the middle of the rear axle, it undergoes a lateral motion of 0.3m, consistent with the lateral deviation noticed in figure 8. The same phenomenon can be observed on the second robot at iteration 450: since the GPS antenna of the second robot is higher (1.8m above the rear axle), its lateral motion is larger (0.4m, as it can be noticed in figure 8). Despite such perturbations and sliding induced by the slope, the proposed formation control is able to preserve the desired formation shape with a high level of accuracy, consistent with farm tasks. The relative lateral accuracy can also be checked in figure 7: besides the reference path, the actual trajectories achieved by the robots are also reported (in blue for the leader and in red for the follower). This illustrates the ability to achieve field covering by a parallel multi-vehicle treatment.

In a such a configuration, the lateral accuracy is the main issue. Nevertheless, the proposed approach aims at

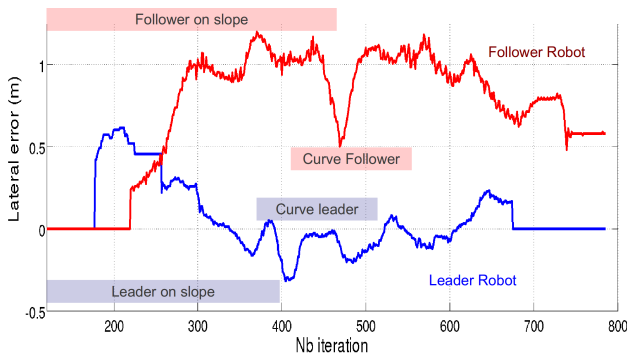


Fig. 8. Comparison of lateral deviations recorded by the two robots

ensuring also a high level of accuracy in longitudinal relative positioning, so that other configurations, such as for instance unloading operations, can be addressed. In order to illustrate longitudinal performances, the curvilinear distance between the 2 robots is depicted in black plain line in figure 9. After the initialization phase, it converges to the desired distance set to 10m. In steady state conditions, high accuracy can be observed (the error does not exceed 20cm). In contrast, in transient phases, such as curvature variations for the second robot at iterations 450 and 650, the accuracy is slightly depreciated: 50cm overshoots can be noticed, due to the settling time of the velocity actuators (the second robot has to change its velocity, since it is supposed to go faster during the curve).

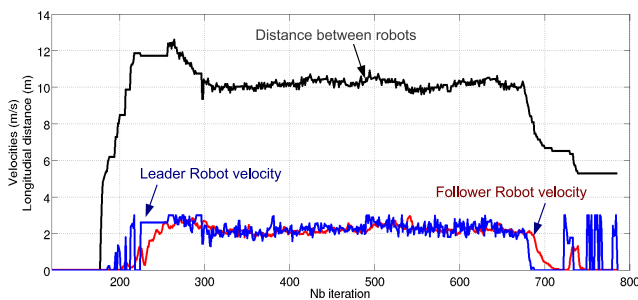


Fig. 9. Curvilinear distance between robots and recorded velocities

In order to investigate further the origin of these overshoots, the robot velocities are reported in figure 9, in blue dotted line for the leader and in red plain line for the follower. It can be seen that the velocity variations in the case of the first robot are more reactive than in the case of the second one. Such a difference induces inaccuracy in longitudinal relative positioning, since, contrarily to lateral motion control, there is no predictive action allowing to anticipate for curvature variations or velocity changes of the first robot. This is especially penalizing when the velocity of the first robot presents large variations: for instance, at the end of the path tracking experimentation (iteration 680), the leader stops abruptly, but the follower takes time to reduce its speed and the longitudinal error eventually exceeds 2m. Such inaccuracies may lead to dangerous situations when robots move fast and/or close to each others. As pointed

out in conclusion and future work, a predictive longitudinal control accounting for other robots control variables is under development.

### C. Traversability results through a sidewalk crossing

In order to illustrate the algorithm proposed to manage traversability, a 15cm high sidewalk has been located on the robot reference path, as depicted in figure 10. Specifically, the reference trajectory crosses the sidewalk right in the middle, and the corridor width is defined as the sidewalk length, so that the selected path has to cross the obstacle. As it can be intuitively noticed in view of figure 10, the



Fig. 10. Experiment investigating traversability problematic

robot is not able to cross safely such a bump at the 1.2 m/s desired velocity. Since this area cannot be avoided, the proposed algorithm for traversability evaluation then computes the velocity profile enabling to cross the bump without breaking the robot (i.e ensuring the maximal pitch velocity of  $0.06\text{rad/s}$ ). The figure 11 shows the computed admissible velocities along the alternative trajectories when the robot is 1.5m before the step.

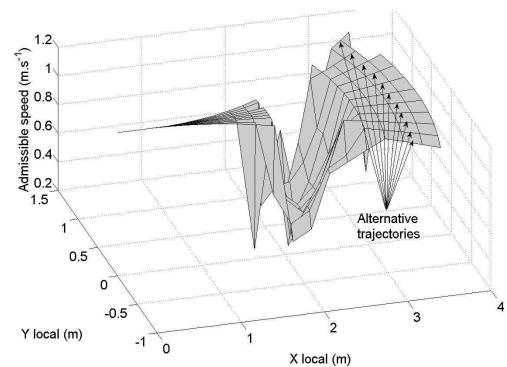


Fig. 11. Results of actual velocity computed when crossing a sidewalk

Since all of trajectories cross the obstacle, each of the velocity profiles reaches the reduced speed of  $0.2\text{m/s}$ . As a result the selected path correspond to the reference trajectory (optimizing the lateral deviation). The actual velocity recorded during the step crossing with respect to the achieved trajectory is depicted on figure 12. As it can be seen, the

robot decreases its speed in order to cross the step at the maximal computed speed of 0.2m/s, showing the relevance of the approach providing a sufficiently accurate digital elevation map.

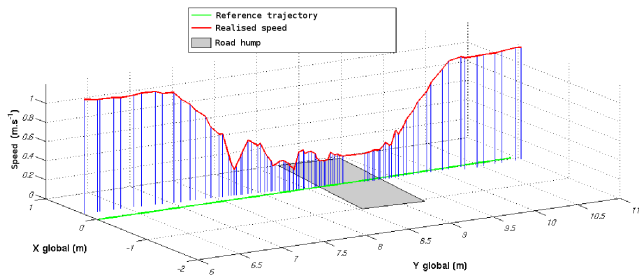


Fig. 12. Results of actual velocity computed when crossing a sidewalk

## V. CONCLUSION AND FUTURE WORK

In this paper, an algorithm dedicated to high accurate and safe formation control for off-road mobile robots is proposed. It is based on a path tracking framework and relies on an adaptive approach taking advantages of an extended kinematic model. Specifically, lateral and longitudinal dynamics are decoupled and the effects of bad grip conditions can be accounted. In addition, predictive techniques applied to lateral motion control enable to anticipate for fast curvature variations. As a result, a high accuracy in the relative position of the robots can be obtained, allowing to preserve the formation shape whatever the grip conditions and the overall desired motion (i.e. the geometry of the reference trajectory). The integrity of each robot is addressed thanks to an algorithm investigating the capability of each robot to cross an area. More precisely, the maximal admissible velocity along possible trajectories is computed relying on a digital elevation map of the terrain in front of the robot. Due to limitations in the available perception system, experimental results related to formation control and traversability preservation are presented separately. Nevertheless, the capabilities of each part of the controller are investigated through actual trials achieved in full scale conditions. The results obtained are consistent with farmer expectations and demonstrate the capability of achieving actual agricultural tasks.

The current development aims at implementing an elevation map reconstruction device on each robot in order to perform a complete evaluation of the proposed approach, i.e. enabling a formation to cross a given area. Obstacle avoidance will then have to take into account the multi-robot problematic. A competition between formation servoing and uncrossable area avoidance will have to be addressed (e.g. either the robots maintain the formation shape when avoiding the area, or the formation shape is transiently altered in order to avoid the area). The alternative path generation described in this paper then needs to be extended to select the best strategy according to the context. Beyond security aspects, the elevation map available on each robot may also be used by these latter to estimate the positions of the others (only

known by wireless communication in this paper). As a result, formation control may become tolerant to communication losses, which is not the case today.

Current work is also focused on robot speed increase, implying to extend predictive techniques, here applied only to lateral motion control, to longitudinal control. As pointed out in section IV, longitudinal errors may present some overshoots due to the settling time of the velocity actuator (a priori specific to each robot). The size of the overshoots naturally depends on the current velocities and may not be acceptable in some applications.

The use of additional robot variables together with partial dynamic models (as achieved in [21] for lateral motion control) are investigated in order to improve the formation control reactivity. The velocity increase also requires to address dynamic stability, as well as controllability, preservation (e.g. avoiding spin around situations). This must be accounted in the evaluation of traversability. Just as for formation shape management, a high level supervisor has also to be proposed to complete the algorithm. It will permit to check the admissibility of the desired configurations, pending on the task and the current state of the formation, and ensure the security level required for actual field applications. Such an improvement should then permit to achieve completely autonomous applications, meeting the farmers expectations, and improving the quality of agricultural and environmental activities.

## REFERENCES

- [1] C. Canudas de Wit, G. Bastin, and B. Siciliano, *Theory of Robot Control*. Springer-Verlag, New York, USA, 1996.
- [2] T. Balch and R. Arkin, "Behavior-based formation control for multi-robot teams," *IEEE Transactions on Robotics and Automation*, vol. 14(6), pp. 926–939, 1998.
- [3] J. Desai, J. Ostrowski, and V. Kumar, "Controlling formations of multiple mobile robots," in *IEEE International Conference on Robotics and Automation (ICRA)*, Leuven (Belgium), 1998, pp. 2864–2869.
- [4] Y. Cao, A. Fukunaga, and A. Kahng, "Cooperative mobile robotics: Antecedents and directions," *Autonomous Robots*, vol. 4(1), pp. 7–27, 1997.
- [5] S. Blackmore, B. Stout, M. Wang, and B. Runov, "Robotic agriculture - the future of agricultural mechanisation?" *5th European Conference on Precision Agriculture (ECPA)*, Upsala (Sweden), 2005.
- [6] E. Sahin, "Swarm robotics: from sources of inspiration to domains of application," *Swarm Robotics, Proceedings of the SAB 2004 International Workshop, Lecture Notes in Computer Science*, 2004.
- [7] J. Fax and R. Murray, "Information flow and cooperative control of vehicle formations," *IEEE Transactions on Automatic Control*, vol. 49(9), pp. 1465–1476, 2004.
- [8] H. Yamaguchi, T. Arai, and G. Beni, "A distributed control scheme for multiple robotic vehicles to make group formations," *Robotics and Autonomous Systems*, vol. 36(4), pp. 125–147, 2001.
- [9] R. Simmons, "The curvature-velocity method for local obstacle avoidance," in *IEEE International Conference on Robotics and Automation*, Minneapolis, MN (USA), 1996.
- [10] D. Fox, W. Burgard, and S. Thrun, "The dynamic window approach to collision avoidance," *IEE Robotics and Automation Magazine*, vol. 4, no. 1, pp. 23–33, 1997.
- [11] C. Debain, P. Delmas, R. Lenain, and R. Chapuis, "Integrity of an autonomous agricultural vehicle according the definition of trajectory traversability," in *Ageng 2010, International Conference on Agricultural Engineering*, 06/09/2010, Clermont-Ferrand, France, 2010.
- [12] C. Samson, "Control of chained systems. application to path following and time-varying point stabilization of mobile robots," *IEEE Transactions on Automatic Control*, vol. 40(1), pp. 64–77, 1995.



- [13] C. B. Low and D. Wang, "Robust path following of car-like WMR in the presence of skidding effects," in *IEEE International Conference on Mechatronics*, 2005, pp. 864–89.
- [14] F. Ben Amar and P. Bidaud, "Dynamic analysis of off-road vehicles," in *Intern. Symp. on Experimental Robotics*, Stanford, U.S.A., 1995.
- [15] R. Lenain, B. Thuilot, C. Cariou, and P. Martinet, "High accuracy path tracking for vehicles in presence of sliding: Application to farm vehicle automatic guidance for agricultural tasks," *Autonomous Robots*, vol. 21(1), pp. 79–97, 2006.
- [16] C. Cariou, R. Lenain, B. Thuilot, and M. Berducat, "Automatic guidance of a four-wheel-steering mobile robot for accurate field operations," *Journal of Field Robotics*, vol. 26(6-7), pp. 504–518, 2009.
- [17] J. Bom, B. Thuilot, F. Marmoiton, and P. Martinet, "A global control strategy for urban vehicles platooning relying on nonlinear decoupling laws," in *IEEE/RSJ International Conference on Intelligent Robots and Systems (IROS)*, Edmonton (Canada), 2005, pp. 2875–2880.
- [18] P. Morin and C. Samson, "Commande de véhicules sur roues non holonomes, une synthèse." in *Actes des troisièmes journées nationales de la recherche en robotique (JNRR)*, Giens (France), 2001.
- [19] R. Lenain, J. Preynat, B. Thuilot, P. Avanzini, and P. Martinet, "Adaptive formation control of a fleet of mobile robots: application to autonomous field operations," 2010, pp. 1241–1246.
- [20] F. Malartre, P. Delmas, R. Chapuis, and C. Debain, "Real-time dense digital elevation map estimation using laserscanner and camera slam process," 2010, pp. 1212–1218.
- [21] R. Lenain, B. Thuilot, C. Cariou, and P. Martinet, "Mixed kinematic and dynamic sideslip angle observer for accurate control of fast off-road mobile robots," *Journal of Field Robotics*, vol. 27, no. 2, pp. 181–196, 2010.